Two-pulse driving of D+D nuclear fusion within a single Coulomb exploding nanodroplet

Isidore Last,[1] Fabio Peano,[2] Joshua Jortner,[1] and Luis O. Silva[2]
[1]*School of Chemistry, Tel Aviv University, Ramat Aviv, 69978 Tel Aviv, Israel*
[2]*GoLP/Instituto de Plasmas e Fusão Nuclear, Instituto Superior Técnico, 1049-0001 Lisboa, Portugal*

(Received 15 October 2009; accepted 6 January 2010; published online 24 February 2010)

This paper presents a computational study of D+D fusion driven by Coulomb explosion (CE) within a single, homonuclear deuterium nanodroplet, subjected to double-pulse ultraintense laser irradiation. This irradiation scheme results in the attainment (by the first weaker pulse) of a transient inhomogeneous density profile, which serves as a target for the driving (by the second superintense pulse) of nonuniform CE that triggers overrun effects and induces intrananodroplet (INTRA) D+D fusion. Scaled electron and ion dynamics simulations were utilized to explore the INTRA D+D fusion yields for double-pulse, near-infrared laser irradiation of deuterium nanodroplets. The dependence of the INTRA yield on the nanodroplet size and on the parameters of the two laser pulses was determined, establishing the conditions for the prevalence of efficient INTRA fusion. The INTRA fusion yields are amenable to experimental observation within an assembly of nanodroplets. The INTRA D+D fusion can be distinguished from the concurrent internanodroplet D+D fusion reaction occurring in the macroscopic plasma filament and outside it in terms of the different energies of the neutrons produced in these two channels. © *2010 American Institute of Physics*. [doi:10.1063/1.3309482]

I. INTRODUCTION

Molecular clusters and nanodroplets (CaNs) interacting with ultraintense and ultrashort near-infrared laser pulses (peak intensities of $10^{15}-10^{21}$ W cm^{-2} and a pulse length of 10–1000 fs) undergo extreme multielectron ionization followed by Coulomb explosion (CE), with the production of high-energy (keV to MeV), highly charged ions or/and nuclei.[1–3] Upon a proper choice of the laser parameters (pulse shape/train and intensity[1–3]), the CaN composition,[2–7] the size,[2,4–7] and the density profile,[8–10] the nuclei produced by CE attain sufficiently high energies to drive table-top nuclear fusion and nucleosynthesis, i.e., D+D,[4,5,11–17] D+T,[7,15] and H+A (A=C,N,O) (Ref. 6) reactions. The driving of D+D fusion for table-top neutron sources was experimentally demonstrated by CE of deuterium containing homonuclear $(D_2)_N$ clusters,[4,12] heteronuclear $(CD_4)_N$ clusters,[11,12] and $(D_2O)_N$ CaNs,[13,14] in accord with theoretical-computational studies.[2,5–7,15–19]

Experimental and theoretical studies of nuclear reactions driven by CE of CaNs focused on inter-CaN (INTER) reactions, which occur between nuclei produced from different CaNs.[1,2,4–6,11–19] Recent theoretical-computational studies predicted that table-top fusion and nucleosynthesis can also be generated by intra-CaN (INTRA) collisions between nuclei (or ions) within a single Coulomb exploding CaN.[3,7–10,20,21] The INTRA reactions driven by CE within a single nanodroplet extend the research area of single molecule[22] and single protein[23] spectroscopy and dynamics to the realm of nanoscience, encompassing CE dynamics within a single nanostructure.

Due to near-spherical symmetry of CE of CaNs, a necessary condition for the occurrence of INTRA reactions rests on the prevalence of overrun effects, which trigger nonuniform CE. Indeed, kinematic overrun effects[5,15,20,21] are ubiquitous in nonuniform CE of heteronuclear CaNs, e.g., $(DT)_N$ or $(CH_4)_N$.[7] For a homonuclear CaN, e.g., $(D_2)_N$, with a homogeneous, steplike initial density profile, CE is uniform under the conditions of cluster vertical ionization (CVI) by a single laser pulse,[3,6–8,24] and INTRA reactions are precluded. Kaplan *et al.*[8] and Peano *et al.*[9,10,20] showed that inhomogeneous initial density profiles of nuclei/ions in homonuclear clusters result in nonuniform CE, which can drive INTRA collisions between identical nuclei. How can an "initial" inhomogeneous density profile (distribution) be produced within a homonuclear cluster? Peano *et al.*[9,10,20] proposed and showed that density profiles that decrease smoothly with increasing r can be produced by a two-pulse irradiation scheme, with the first weaker pulse being followed by a second strong pulse. The feasibility and effectiveness of this scenario for $(D_2)_N$ were demonstrated by Peano *et al.*[9,10] by two-dimensional and three-dimensional (3D) massively parallel, relativistic, electromagnetic particle-in-cell (PIC) simulations within the OSIRIS 2.0 framework,[9,10,25] providing preliminary estimates of INTRA D+D fusion yields.

In this paper we apply the recently developed method of scaled electron and ion dynamics (SEID) 3D molecular dynamics (MD) simulations[7,26] to explore the D+D fusion yields for INTRA processes driven by double-pulse near-infrared laser irradiation of a $(D_2)_N$ nanodroplet. Our SEID results provide information on the dependence of the D+D fusion yield on the nanodroplet size and on the laser parameters for double-pulse driving of an efficient INTRA D+D [i.e., ^{2}D(d,n)^{3}He and ^{2}D(d,p)^{3}T] fusion. In the nonuniform CE of homonuclear CaNs, the collision energies (which are determined by the difference between the velocities of the overrunning nuclei) are considerably lower than the particle

energies. Accordingly, for INTRA fusion one needs very high (MeV) deuteron energies, which considerably exceed the energies required for the INTER reaction. The attainment of these very high energies for INTRA fusion requires the use of large nanodroplets (with initial radii of $R_0 = 500-3000$ Å), whose maximal CE energies under CVI conditions[2,5,6] correspond to the MeV domain.[7]

II. INTRA D+D FUSION DRIVEN BY COULOMB EXPLOSION OF DEUTERIUM NANODROPLETS

We studied INTRA collisions and the D+D fusion reaction in $(D_2)_N$ nanodroplets driven by a sequential excitation by two Gaussian laser pulses.[9,10] The peak intensity I_1 and the temporal width τ_1 of the first pulse are chosen to accomplish complete inner ionization, while the outer ionization process removes only a small fraction of the nanoplasma electrons. The resulting persistent, "cold" nanoplasma[27,28] fills an inner part of the nanodroplet volume. Consequently, the nanodroplet consists of a central neutral sphere and a positively charged ionized outer periphery shell.[10,20] The charged periphery shells undergo CE, forming an expanding nanodroplet with an inhomogeneous density profile, which decreases toward the boundary.[9,10,20,29] The exploding nanodroplet with an inhomogeneous density profile is subsequently irradiated by a considerably more intense second pulse with a peak intensity of I_2 and a temporal width of τ_2, being switched on at a time delay t_{12} ($t_{12} \geqslant \tau_1, \tau_2$) relative to the peak of the first pulse. The second pulse triggers complete outer ionization of the persistent nanoplasma [on the time scale of $(t_{12}-\tau_2)\cdots t_{12}$], inducing effective CE of the inhomogeneous structure of the bare nuclei. Accordingly, two-pulse irradiation of the homonuclear nanodroplet drives nonuniform CE, with the velocities of the ions from the central domain being higher than those from the periphery. Figure 1 demonstrates the prevalence of overrun effects for the trajectories of deuteron pseudoparticles,[26] initially located at different distances from the nanodroplet center. These were obtained from SEID MD simulations (Refs. 7 and 26 and Sec. III below) for double-pulse driving of a $(D_2)_N$ nanodroplet ($R_0 = 1150$ Å, $N = 1.36\times10^8$). The trajectories r(t) of ions from the vicinity of the nanodroplet periphery exhibit a marked increase throughout the first pulse (Fig. 1), manifesting CE of the positively charged outer nanodroplet domain. In contrast, the trajectories of the ions initially located in the central neutral region of the nanodroplet exhibit very weak time dependence during the first laser pulse, when CE is precluded, and start a sharp rise only with the switching on of the second pulse. The attainment of higher velocities of the central ions relative to the periphery ions during the second pulse results in the crossover of their trajectories (Fig. 1) with the formation of multiple ion flows, which were referred to as "shock shells."[8–10,30] These multiple flow regions provide a medium for D+D collisions and fusion.[8–10] Indeed, the D+D differential fusion yield [Eq. (2) and Sec. III below] is maximized in the time domain for the crossing of trajectories (Fig. 1). Following our previous analysis,[29] it will be appropriate to refer to these multiple flow regions as "overrun shells." As shown in the Appendix, the overrun

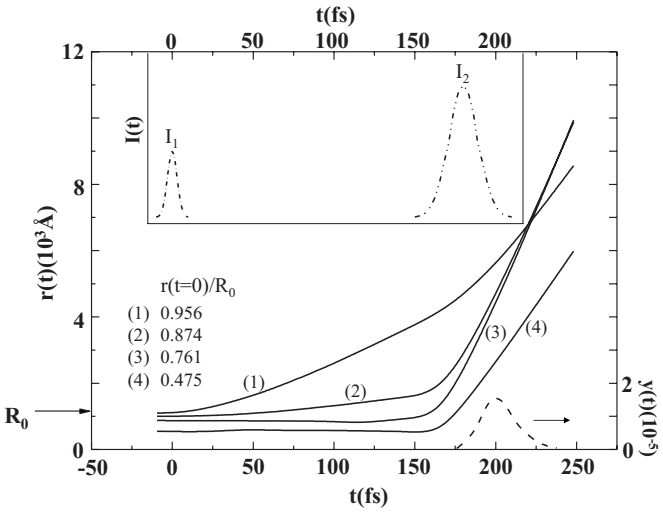

FIG. 1. SEID MD simulations (with a scaling parameter $s=4\times10^4$) of trajectories of deuteron pseudoparticles for double-pulse driving of a $(D_2)_N$ nanodroplet with an initial radius of $R_0=1150$ Å ($n=2N=2.72\times10^8$). The laser parameters of the first pulse are $I_1=10^{17}$ W cm^{-2} and $\tau_1=10$ fs, while for the second pulse $I_2=10^{20}$ W cm^{-2} and $\tau_2=30$ fs. The trajectories r(t) present the radial distance of the center of a pseudoparticle from the nanodroplet center at time t, with the initial distance r(t=0). The trajectories (solid lines) are specified by the values of $r(t=0)/R_0$ presented in the figure. Trajectory (1) originates from the vicinity of the nanodroplet periphery, while trajectories (3) and (4) originate from the central regions of the nanodroplet. The dashed curve in the lower right-hand side represents the D+D differential fusion yield y(t) [calculated by SEID simulations using Eqs. (1)–(5)], which is appreciable in the time domain for the crossing of trajectories from the periphery and from the central nanodroplet regions. The inset shows the laser parameters for the two Gaussian pulses, represented on an arbitrary scale.

shells are produced not only in nanodroplets (Fig. 1), but also in intermediate size clusters.

The total yield for INTRA D+D fusion driven by CE of a single $(D_2)_N$ nanodroplet (per sequence of two laser pulses) is[7]

$$Y = \int_{t_{on}}^{\infty} y(t)dt, \tag{1}$$

where y(t) is the differential fusion yield (per time unit) and t_{on} is the onset time of the second laser pulse (see Sec. III). In a previous work,[7] where pure ionic nanodroplets were mainly considered, the differential yield was presented in the spherical symmetry approximation. In the presence of nanoplasma electrons, the spherical symmetry of the ions (nuclei) expansion can be violated, with the motion of the electrons being of cylindrical symmetry along the laser field polarization axis.[28] The differential reaction yields y(t) between identical nuclei were calculated by performing an integration for a cylindrical symmetry being presented in the form

$$y(t) = (1/2)2\pi\int_0^{R(t)} r^2\rho(r,t)dr\int_0^{\pi}\rho(\alpha;r,t)\zeta(\alpha,r,t)\sin(\alpha)d\alpha, \tag{2}$$

where R(t) is the nanodroplet radius at time t, α is the angle between the radius vector **r** and the laser field polarization axis, $\rho(\alpha;r,t)$ is the local density of nuclei at $\vec{r}$, $\rho(r,t)$ is the

density of nuclei at the distance r from the nanodroplet center averaged over α [with the possible differences between $\rho(\alpha;r,t)$ and $\rho(r,t)$ being due to local fluctuations], $\zeta(\alpha,r,t)=\langle\sigma v\rangle$ is the product of the reaction cross section σ (Ref. 31) and the center of mass (CM) collision velocity v averaged over the CM energy E′ distribution $P(E';\alpha,r,t)$, so that

$$\zeta(\alpha,r,t)=\int_0^\infty P(E';\alpha,r,t)\sigma(E')v(E')dE'. \quad (3)$$

In the laboratory frame, the CM energy E'_{ij} and the velocity v_{ij} for radial ion motion are expressed in the form

$$E'_{ij}=\tfrac{1}{2}(E_i^{1/2}-E_j^{1/2})^2, \quad (4)$$

$$v_{ij}=\frac{\sqrt{2}}{m_D}(E_i^{1/2}-E_j^{1/2}), \quad (5)$$

with i and j indicating the ions with the energies E_i and E_j, respectively, and $E_i>E_j$.

III. SCALED MOLECULAR DYNAMICS SIMULATIONS

The large nanodroplet size ($\sim 10^7-10^9$ D atoms) for which INTRA reactions occur precludes the use of the traditional MD simulations. Data for the time-dependent local density $\rho(\alpha,r,t)$, the energy distribution $P(E';\alpha,r,t)$, and the velocities v(E′), which determine the INTRA reaction yield [Eqs. (1)–(5)], were obtained from the SEID simulations.[26] The SEID considers MD in a scaled nanodroplet with a reduced number of composite particles (i.e., pseudoelectrons and pseudoions/nuclei), scaled initial interpseudoparticle distances, and scaled short-range potential parameters.[26] A single scaling parameter s ($\gg 1$) is used that accounts for the composition, mass, and charge of all the pseudoparticles, while the initial distances between the pseudoparticles are scaled by $s^{1/3}$. SEID simulations for nanodroplet CE in an ultraintense laser field are based on standard MD simulations for the pseudonanoparticles.[26] Relativistic effects[26,32,33] were included in the SEID simulations. As discussed in Ref. 26, the validity conditions for the accuracy of the SEID method are (1) the dominance of long-range Coulomb interactions, which ensure nearly identical accelerations and trajectories of the nanodroplet particles and of the composite pseudoparticles, and (2) the proper choice of the scaling parameters, which is chosen to guarantee the near independence of the energetic parameters on s.

We utilized SEID for the simulation of a laser driven $(D_2)_N$ nanodroplet with the initial radii $R_0=600-1400$ Å (number of deuterons $n=2N=4.34\times10^7-5.53\times10^8$). The first Gaussian laser pulse was characterized by a frequency of $\nu_1=0.35$ fs^{-1}, peak intensities in the range of $I_1=10^{15}-10^{18}$ W cm^{-2}, and pulse widths of $\tau_1=10-40$ fs. The first laser pulse (with its peak being located at t=0) was switched on at $t_s=-\tau_1$.[32] At t_s complete inner ionization of the deuterium nanodroplet occurs.[32] The initial nuclear configuration of the n=2N ions was described by a homogeneous distribution, which provides the initial atomic density $\rho=0.05$ Å^{-3} of the deuterium nanodroplet. This ion structure, together with the n=2N electrons, forms the nanoplasma.[26,32] The deuterons and the electrons were used to construct the pseudoparticles used in the SEID scheme.[26] In the range of the first pulse parameters used herein, the completely inner-ionized nanodroplet undergoes partial outer ionization.[27,29,32,34] The second Gaussian laser pulse was characterized by the same frequency with a peak intensity of $I_2=10^{20}$ W cm^{-2} and a pulse width of $\tau_2=20-30$ fs. This second pulse provides complete outer ionization of the nanodroplet. The simulations were performed for the second laser pulse delay in the range of $t_{12}=110-180$ fs, with the delay time being determined as the temporal distance between the two pulse peaks. For t_{12} values Y increases in this domain with increasing t_{12} in the range of 110–150 fs and then reaches near saturation for $t_{12}=150-180$ fs. The value of $t_{12}=180$ fs is roughly optimal for the maximization of the fusion yields. The optimal values of τ_1 and τ_2 for the attainment of maximal yields were calculated in the τ_1, τ_2 range given above. For example, SEID simulations (with $s=7\times10^4$) for $R_0=1100$ Å, with the laser parameters $I_1=10^{17}$ W cm^{-2}, $I_2=10^{20}$ W cm^{-2}, $\tau_2=30$ fs, and $t_{12}=180$ fs, revealed a maximum of $Y=5.0\times10^{-3}$ at $\tau_1=10$ fs, with a decrease to $Y=1.6\times10^{-4}$ at $\tau_1=30$ fs, while the yields show a small variation with the change in τ_2. These optional τ_1 and τ_2 data are presented in Table I.

IV. INTRA D+D FUSION YIELDS

SEID simulations were performed for the R_0 values given in Table I, with the scaling parameters being varied in the range $s=5\times10^3-2\times10^4$ for $R_0=600$ Å ($n=4.3\times10^7$) up to $s=4\times10^4-1\times10^5$ for $R_0=1400$ Å ($n=5.5\times10^8$). It will be useful to provide normalized values, (s/n), for the presentation of the scaling parameters. The SEID simulations were performed for this normalized parameter in the range $(s/n)=7\times10^{-5}-1.8\times10^{-4}$ for $R_0=800-1400$ Å and $(s/n)=1\times10^{-4}-4.5\times10^{-4}$ for $R_0=600$ Å (Fig. 2). This normalized parameter is inversely proportional to the number $\tilde{n}=(n/s)$ of the deuteron pseudoparticles,[26] i.e., $\tilde{n}\simeq2\times10^3-1.5\times10^4$ in our SEID simulations. With our computational setup[32,33] using the CPU of a Silicon Graphics Origin 3200, Itanium-2, 1784 MHz machine, the choice of the lowest value of (s/n) is limited by the computational time of ~45 d for $(s/n)\approx6\times10^{-5}$ for the largest nanodroplets used herein, i.e., $s=4\times10^4$ for $R_0=1400$ Å and $s=1.8\times10^4$ for $R_0=1100$ Å. For fixed values of the double-pulse parameters, the final CE kinetic energies of the deuterons were found to be weakly sensitive to s (i.e., changing only in the range of 15%–20%) in the s domain used herein. The near saturation of the CE energies and other single-particle kinematic parameters in this s domain concurs with the validity condition for the convergence of the SEID results to the ordinary MD data for the kinetic energies, which is valid for $\tilde{n}>200$,[26] i.e., $s/n=1/\tilde{n}<5\times10^{-3}$. This validity condition is well satisfied for all the values of (s/n) used herein (Fig. 2). In contrast to the CE kinetic energy data, which nearly converge in the s domain used here, we found that the fusion yields, Eqs. (1)–(5), which are determined by the two-particle CM energies in the laboratory frame, exhibit a some-

TABLE I. The nanodroplet size dependence of the optimal values of the temporal pulse widths τ_1 and τ_2 at several fixed values of the intensity I_1 for the first pulse (with $t_{12}=180$ fs and $I_2=10^{20}$ W cm^{-2}), which are required for the attainment of maximal values of the INTRA D+D fusion yields. The INTRA yields were obtained from SEID simulations (Fig. 2) by three procedures (see text): (i) Y at $s=s_{min}$; (ii) Y obtained from two-point extrapolation to s=1 ((s/n)→0); and (iii) Y obtained from three-point extrapolation to s=1 ((s/n)→0).

R_0 (Å)	n	I_1 (W cm^{-2})	τ_1 (fs)	τ_2 (fs)	Y (i)	Y (ii)	Y (iii)
600	4.34×10^7	10^{15}	20	20	4.16×10^{-5}	1.80×10^{-5}	1.82×10^{-5}
		10^{16}	20	20	7.17×10^{-5}	5.85×10^{-5}	5.85×10^{-5}
800	1.09×10^8	10^{16}	25	30	4.33×10^{-4}	4.04×10^{-1}	3.42×10^{-4}
1100	2.68×10^8	10^{16}	30	30	3.04×10^{-3}	2.19×10^{-3}	2.70×10^{-3}
		10^{17}	10	30	3.12×10^{-3}	2.88×10^{-3}	2.81×10^{-3}
1400	5.53×10^8	10^{17}	15	20	1.81×10^{-2}	1.48×10^{-2}	1.60×10^{-2}

what stronger dependence on the scaling parameter. As is apparent from Fig. 2, the calculated fusion yield Y(s) [i.e., the yield calculated from Eq. (1) at the value of s] decreases with decreasing s for all values of the nanodroplet radii (R_0) and of the first pulse parameters (I_1). For nanodroplets in the size domain $R_0=600-1400$ Å driven by $I_1=10^{16}$ W cm^{-2} and 10^{17} W cm^{-2}, Y(s) decreases by a numerical factor of ~2 or less with decreasing (s/n) in the range $(s/n)=1.8\times10^{-4}-7\times10^{-5}$ (Fig. 2). For $R_0=600$ Å and $I_1=10^{15}$ W cm^{-2} the yields Y(s) decrease by a numerical factor of ~3 in this (s/n) range (Fig. 2). Three procedures for estimates of the INTRA fusion yields (at s=1) were advanced and are presented in Table I. (i) An upper limit for Y was estimated as $Y(s_{min})$, where s_{min} corresponds to the lowest scaling parameter used in the simulation. (ii) A two-point extrapolation. The Y(s) data for the two lowest s values were linearly extrapolated by $Y(s)=Y+as$ to s=1 (or rather to $s/n=0$ as $1/n\ll1$). (iii) A three-point extrapolation. The Y(s) data for the three lowest s values were extrapolated to s=1 (or rather to s/n=0) by $Y(s)=Y+as+bs^2$. The three procedures for the estimates of Y (Table I) reveal that $Y(s_{min})$ [procedure (i)] exceeds the extrapolated data [procedures (ii) and (iii)] by a numerical factor of ~2, or less, while the results of the two extrapolation methods [procedures (ii) and (iii)] do not differ by more than 25%. In what follows, we shall use the estimates for Y based on the extrapolation method (iii). In view of the empirical nature of the extrapolation methods, we assert that these estimates of Y are reliable within the range of 20%–50%, being adequate for the subsequent analyses of size and laser parameter dependence of the INTRA yields. This accuracy is sufficient for the sake of predictions and future analyses of experimental data for INTRA fusion. A final comment will be in order regarding the applicability of our empirical extrapolation of the SEID data for the estimates of the INTRA fusion yields (for s=1) within Coulomb exploding $(D_2)_N$ nanodroplets (with $n=4.3\times10^7-5.5\times10^8$, where n=2N). For the large nanodroplets used herein the calculation of the INTRA yields for s=1 by the standard MD method is not feasible. Such MD simulations (for s=1) can be performed only for small or intermediate size clusters (e.g., $n=2N\lesssim1.3\times10^4$), for which the center of energies of the colliding ions, Eq. (4), is too small to generate any noticeable INTRA fusion yields (see the Appendix). We shall specify the INTRA D+D collisions in intermediate size clusters in terms of the CM collision energies. We performed MD simulations (for s=1) and SEID simulations (for s=2–16) for the CM kinetic energies within $(D_2)_N$ clusters (with $n=1.3\times10^4$ and $R_0=40$ Å), establishing the convergence of the SEID data (see the Appendix). These SEID data converge to the s=1 results for s=8–4, i.e., $s/n\lesssim3\times10^{-4}$, where n=2N (see the Appendix). The convergence of the SEID method for the CM collision kinetic energy for intermediate size clusters is manifested for $s/n\lesssim3\times10^{-4}$, with this value of s/n being in semiquantitative agreement with the empirical convergence of Y(s) in nanodroplets (in the range $s/n=4.5\times10^{-4}-1.0\times10^{-4}$, Fig. 2). These MD and SEID simulation data for medium-sized

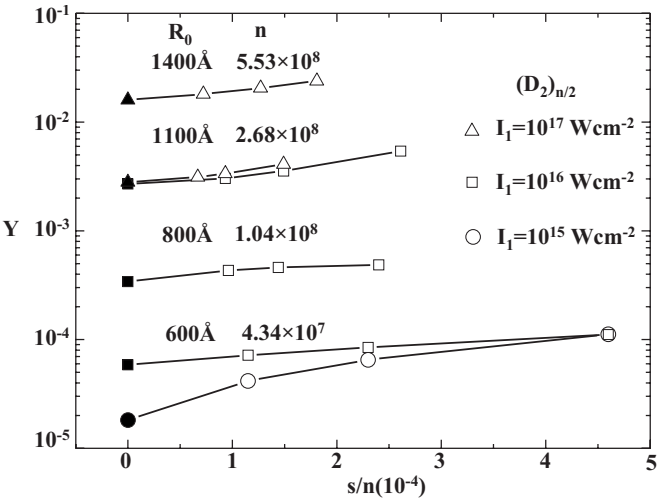

FIG. 2. SEID simulations for the INTRA D+D fusion yields from a $(D_2)_N$ nanodroplet driven by two-pulse irradiation by two Gaussian laser pulses. The simulation results are represented by open symbols for the nanodroplet sizes marked on the curves. The laser temporal widths were taken from Table I. The second laser pulse was characterized by $I_2=10^{20}$ W cm^{-2} and $t_{12}=180$ fs. The peak intensities I_1 of the first pulse are represented by different symbols as marked in the figure. The solid lines represent the three-point extrapolation of the SEID simulation results, according to the relation $Y(s)=Y+as+bs^2$ [procedure (iii) in the text]. The black symbols represent the extrapolated INTRA fusion yield Y data for $I_1=10^{17}$ W cm^{-2} (▲), $I_1=10^{16}$ W cm^{-2} (■), and $I_1=10^{15}$ W cm^{-2} (●).

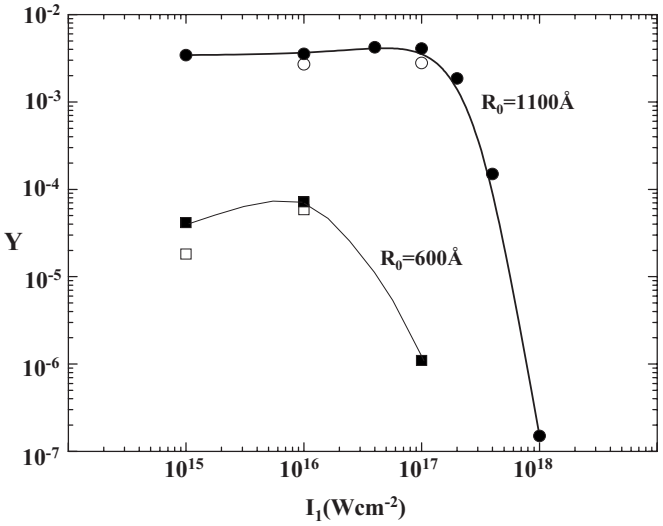

FIG. 3. The dependence of the single nanodroplet INTRA D+D fusion yield on the intensity of the first pulse for large (R_0=1100 Å) and smaller (R_0=600 Å) nanodroplets. The data for R_0=1100 Å were taken from procedure (iii) in Table I (○) and from SEID simulations with $s=4\times10^4$ (●). The data for R_0=600 Å were taken from procedure (iii) in Table I (□) and from SEID simulations with $s=10^4$ (■). The solid lines were drawn to guide the eye.

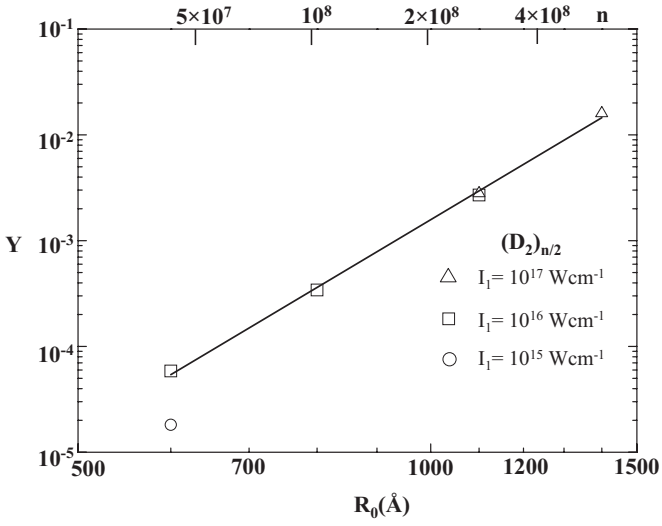

FIG. 4. The nanodroplet size (R_0) dependence of the single-nanodroplet INTRA D+D fusion yield for the intensities $I_1=10^{17}$ W cm^{-2} (△) and $I_1=10^{16}$ W cm^{-2} (□). Data from Table I. The straight solid line represents the scaling law, Eq. (6a), with α=6.6.

clusters provide strong support for the validity of our SEID scheme for large nanodroplets.

Of considerable interest is the choice of the laser parameters and the nanodroplet size for the attainment of an efficient INTRA yield. For a very large nanodroplet (R_0=1100 Å) the optimal choice of the intensity of the first pulse corresponds to $I_1=10^{15}-10^{17}$ W cm^{-2}, with Y being weakly dependent on I_1 in that intensity range (Fig. 3). Increasing I_1 to 10^{18} W cm^{-2} showed very low fusion yields ($Y<10^{-6}$). The sharp three to four orders of magnitude decrease in Y (for R_0=1100 Å) in the intensity range $I_1=10^{17}-10^{18}$ W cm^{-2} (Fig. 3) is due to the enhancement of outer ionization of the nanoplasma by the first pulse. A similar qualitative trend in the dependence of Y on I_1 is manifested for smaller (R_0=600 Å) nanodroplets, where Y attains a maximum at $I_1=10^{16}$ W cm^{-2}, followed by a sharp two orders of magnitude drop in the range $I_1=10^{16}-10^{17}$ W cm^{-2} (Fig. 3). As the outer ionization yield driven by the first pulse is determined by $I_1^{1/2}/R_0$,[29,35] we expect that the drop in Y is exhibited at lower values of I_1 for R_0=600 Å than for R_0=1400 Å, in accord with the simulation data (Fig. 3). The maximal values of Y exhibit an increase by a numerical factor of ~300 with increasing R_0 from 600 to 1400 Å (Fig. 4), manifesting a sharp nanodroplet size dependence of the yields. In Fig. 4 we portray the dependence of Y on R_0 for the intensities $I_1=10^{16}$ W cm^{-2} and $I_2=10^{17}$ W cm^{-2}. The simulation data for Y at R_0=1100 Å nearly coincide for $I_1=10^{16}$ W cm^{-2} and $I_1=10^{17}$ W cm^{-2} (Fig. 4), reflecting on the flat intensity domain for which Y is maximized (Fig. 3). In the parameter range considered, the nanodroplet size dependence of the INTRA fusion yields (Fig. 4) is well expressed by the (divergent) scaling laws

$$Y = AR_0^{\alpha}; \quad \alpha = 6.6, \quad A = 2.10\times10^{-23}\ \text{Å}^{-\alpha} \tag{6a}$$

and

$$Y = Bn^{\beta}; \quad \beta = 2.2, \quad B = 7.8\times10^{-22}. \tag{6b}$$

This size dependence of Y is determined by several factors involving the variations in the number, the density, and the two-particle CM energies of the deuterons in the multiple flow domains where D+D fusion occurs [Fig. 1 and Refs. 8–10]. The index α=6.6 of Eq. (6a) exceeds the index α=4, which describes the Y dependence on R_0 in the case of constant cross section σ,[10] reflecting an increase in the cross sections with increasing the collision energy within the collision-energy range considered. It is important to note that the superlinear n dependence of the INTRA fusion yields for $R_0\leq1400$ Å implies that the efficiency of INTRA nanodroplet D+D collisions will be markedly enhanced with increasing the nanodroplet size, at least in that size domain.

It will be instructive to confront the present SEID simulation results (for R_0=1100 Å) with the PIC simulations of Peano *et al.*[10,20] for a similar nanodroplet size (R_0=1000 Å). The SEID simulation results of $Y\approx3\times10^{-3}$ for R_0=1100 Å at $I_1=10^{16}-10^{17}$ W cm^{-2} (Table I) are lower by about one order of magnitude than previous estimates obtained with an approximate one-dimensional (1D) model,[10] which give (for R_0=1000 Å) the value of Y=0.03 at $I_1=10^{18}$ W cm^{-2}. The optimal intensities of the first pulse, as determined herein from the SEID simulations, are significantly lower, i.e., by about one order of magnitude, than those obtained with the approximate 1D model used in Ref. 10. Indeed, according to the SEID simulations, the yield for this nanodroplet size was found to be very low at $I_1=10^{18}$ W cm^{-2} (Fig. 3), which is also in agreement with the 3D PIC simulations presented by Peano *et al.*[10]

To assess the possible direct effects of the ultraintense laser fields on ionic motion, we performed SEID simulations

for fusion yield nanodroplets driven by a single-pulse irradiation at $I=10^{20}$ W cm^{-2}, which resulted in negligible fusion yields, providing evidence for the lack of direct laser field effects on the INTRA yields.

V. DISCUSSION

From the foregoing analysis of the Y data for $(D_2)_N$ nanodroplets driven by double-pulse irradiation (Figs. 3 and 4), we shall infer that the INTRA reaction yield per nanodroplet per two-pulse sequence is sufficiently high to warrant experimental observation in an assembly of such nanodroplets. The highest value of the INTRA fusion yield is $Y=1.6\times10^{-2}$ per nanodroplet per two-pulse train for a single nanodroplet with $R_0=1400$ Å (Table I and Fig. 2). The increase in Y by a marked increase in the nanodroplet size will be precluded due to the attenuation of the intensity of the first laser beam within the nanodroplet. This value of Y for a single nanodroplet is too low to allow for experimental observation. The INTRA fusion yield will be amenable to experimental observation within an assembly of nanodroplets. The total INTRA fusion yield Y^{tot}_{INTRA} (per two-pulse sequence) in the reaction volume, which contains N_{nd} nanodroplets, is[7]

$$Y^{tot}_{INTRA}=N_{nd}Y, \tag{7}$$

where

$$N_{nd}=V_f\rho/n, \tag{8}$$

and where ρ is the average ion density in the laser focal volume V_f. From a previous study on $(DT)_n$ nanodroplets under realistic conditions,[7] we take $\rho=2\times10^{18}$ cm^{-3} and $V_f=5\times10^{-7}$ cm^3 and these data are adopted for $(D_2)_N$ nanodroplets. From Eqs. (6b), (7), and (8) we obtain the nanodroplet size dependence of the total INTRA yield

$$Y^{tot}_{INTRA}=BV_f\rho n^{\beta-1}. \tag{9}$$

From the analysis of the Y data (Sec. IV) we inferred that $\beta=2.2$, Eq. (6b), so that $Y^{tot}_{INTRA}\propto n^{1.2}$. In Fig. 5 we present the nanodroplet size dependence of Y^{tot}_{INTRA}, with the laser parameters for each nanodroplet size being taken from Table I to give the maximal value of Y for a given R_0. The sharp increase in Y^{tot}_{INTRA} (Fig. 5) with increasing R_0 is in accord with the scaling relation $Y^{tot}_{INTRA}\propto n^{1.2}\propto R_0^{3.6}$, Eq. (9). Provided that the cross sections were constant, we would expect that $Y^{tot}_{INTRA}\propto R_0$,[10] whereupon the size dependence $Y^{tot}_{INTRA}\propto R_0^{3.6}$ obtained herein reflects an increase in the cross sections with increasing energy.

In considering the experimental implications of the simulation results for Y^{tot}_{INTRA}, we estimate for two-pulse irradiation for an assembly of $(D_2)_N$ nanodroplets that Y^{tot}_{INTRA} rises from 1.4 for $R_0=600$ Å to 29 for $R_0=1400$ Å. These total INTRA fusion yields are amenable to experimental observation. These estimates have to be subjected to experimental scrutiny.

Even if the yield of $D(d,n)^3He$ INTRA reactions is sufficiently high, they have to be distinguished from the yield of $D(d,n)^3He$ INTER reactions taking place in the macroscopic plasma filament and outside of it.[7,36] These two parallel

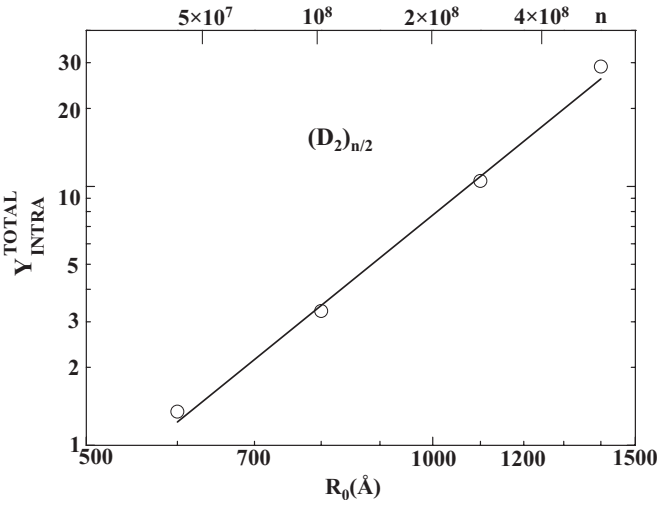

FIG. 5. The nanodroplet size (R_0) dependence of the INTRA fusion yield from an assembly of nanodroplets. Y^{tot}_{INTRA} was calculated from Eq. (7) using the single nanodroplet yield data at the optimal set of the laser pulses' parameters (Table I). The number of the nanodroplets, Eq. (8), was estimated from the data of Ref. 7 (see text). The solid line represents the scaling law $Y^{tot}_{INTRA}\propto R_0^{3.6}$ according to Eq. (9) (see text).

$D(d,n)^3He$ channels produce neutrons in different energy regions. We estimated the neutron energies by using the analysis of Youssef *et al.*,[37] as applied to "forward" and to "backward" collisions. The laboratory energy E_n of the emitted neutron as a function of the incident ion energy E_d is given by[37]

$$E_n^{1/2}=(1/4)\{[2E_d+4(3Q+E_d)]^{1/2}\pm(2E_d)^{1/2}\}, \tag{10}$$

where $Q=3.27$ MeV is the energy release of the $D(d,n)^3He$ reaction,[31] and +(−) refers to forward (backward) collisions. In the limit of low ion energies, $E_d=0$ and the neutron energy is $E_n=2.45$ MeV. For the INTRA reaction mode within an exploding nanodroplet typical deuteron energies, according to our simulations, fall in the range of $E_d=0.1-0.5$ MeV, so that $E_d\ll Q$, and a neutron narrow energy distribution at $E_n=2.45$ MeV will be exhibited. For the INTER reaction mode within and outside the macroscopic plasma filament produced by CE of such nanodroplets, the maximal value of the deuteron energies obtained from our simulations is $(E_d)_{max}\simeq2.5$ MeV (while ion energies in the range of $E_d>2.5$ MeV contribute less than 15%). Using $E_d=2.5$ MeV in Eq. (10), we estimate the neutron energy domain for the INTER reaction mode in the broad range of 1.64 MeV $<E_n<5.76$ MeV. The energy resolution of the neutrons will provide an identification of the INTRA reaction, which results in a narrow neutron energy distribution at $E_n\simeq2.45$ MeV, and which is superimposed on a broad neutron energy distribution $E_n=1.64-5.76$ MeV due to the INTER reaction mode.

An additional diagnostic tool for INTRA and INTER fusion pertains to the distinctive time scales for these two reaction modes. The time scale for the INTRA reaction is $\tau_{INTRA}\approx R/v$, where $R\simeq4000$ Å is the radial distance of the overrun shell within the exploding nanodroplet,[29] and $v\approx10^9$ cm s^{-1} is the velocity of the nuclei, i.e., $\tau_{INTRA}\simeq40$ fs. On the other hand, the time scale for the INTER

reaction, which mainly occurs via collisions of nuclei from the plasma filament with clusters outside it,[35] is in the range of $\tau_{INTER} \approx 2-100$ ps.[36] Accordingly, neutrons from the INTRA reaction with a narrow energy distribution at $E_n = 2.45$ MeV will be emitted in an ultrashort (femtosecond) burst, prior to the appearance of neutrons with the INTER reaction with a broad energy distribution (1.6–5.8 MeV) on the picosecond time scale.

ACKNOWLEDGMENTS

This research was supported by the James-Franck Binational German-Israeli Program on Laser Matter Interaction at Tel Aviv University and by FCT, Portugal through Grant No. PTDC/FIS/66823/2006.

APPENDIX: OVERRUN SHELLS IN INTRA COLLISIONS WITHIN INTERMEDIATE SIZE DEUTERIUM CLUSTERS

The two-pulse irradiation scheme[9,10,20,29] was applied in this paper to large $(D_2)_N$ nanodroplets, where INTRA fusion is generated via the formation of an overrun shell,[29] where multiple flow regions provide a medium for collisions with a high CM energy, resulting in a marked increase in the differential fusion yield y(t), Eq. (2). The overrun shell, which is formed near the periphery of the large nanodroplet, is specified by maxima in the density profile $\rho(r)$ and in the fusion generation function (dy/dr) (Ref. 29). In this appendix we shall demonstrate that the formation of overrun shells by two-pulse irradiation is not limited to large nanodroplets (with $n \approx 10^7-10^8$), which were studied in Secs. III and IV, but can also be manifested in intermediate size clusters ($n \simeq 10^4$). From our analysis of the size scaling of the INTRA fusion yields, Eqs. (6a) and (6b) and Fig. 4, we assert that Y is negligibly small in such intermediate size clusters. The INTRA fusion yield is determined by the CM collision kinetic energy $E_{CM}(r,t)$ for the radial motion of the ions, Eqs. (1)–(5), which is given by

$$E_{CM}(r,t) = [1/2\rho(r,t)] \times \int_0^{\pi} d\alpha \rho(\alpha;r,t) \sin\alpha \int_0^{\infty} dE' P(E';\alpha,r,t) E', \tag{A1}$$

while the averaged CM collision kinetic energy, $\bar{E}_{CM}(t)$, averaged over the cluster volume at time t, is given by

$$\bar{E}_{CM}(t) = 4\pi \int_0^{R(t)} dr r^2 \rho(r,t) E_{CM}(r,t). \tag{A2}$$

The local densities $\rho(\alpha;r,t)$ and $\rho(r,t)$, the nanodroplet radius R(t) at time t, and the distribution function $P(E';\alpha,r,t)$ are defined in Sec. II. Accordingly, the local CM collision kinetic energy $E_{CM}(r,t)$ and the averaged CM collision kinetic energy $\bar{E}_{CM}(t)$ will be used to specify INTRA collisions in intermediate size clusters. $E_{CM}(r,t)$ and $\bar{E}_{CM}(t)$ were obtained from SEID simulations for a $(D_2)_N$ cluster with the initial radius $R_0 = 40$ Å (number of atoms $n = 2N = 1.289 \times 10^4$). The INTRA collisions within this intermediate size cluster can be treated by SEID simulations and also by the standard MD simulations procedure (which is equivalent to the SEID procedure with s=1). These data will allow us to test the convergence of the SEID procedure and assess the validity of the SEID simulation method.

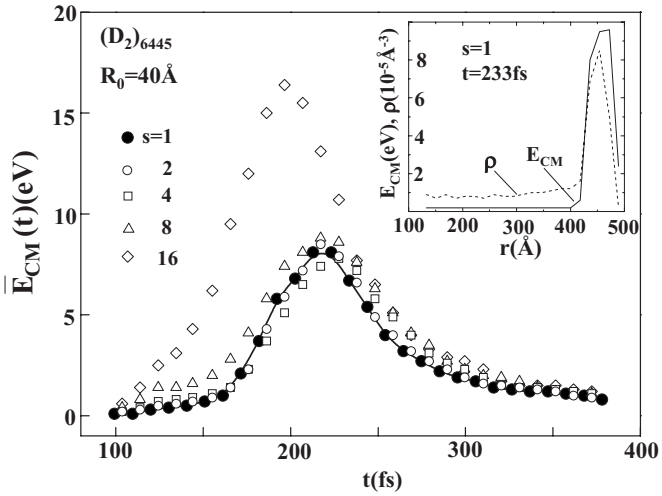

FIG. 6. SEID simulations for the INTRA CM D+D volume averaged collision energy $\bar{E}_{CM}(t)$, Eq. (A2), in an exploding intermediate size $(D_2)_N$ cluster (number of deuterons $n = 2N = 1.289 \times 10^4$ and $R_0 = 40$ Å). The parameters for the two-pulse laser irradiation are $I_1 = 5 \times 10^{14}$ W cm^{-2}, $\tau_1 = 10$ fs, $I_2 = 10^{18}$ W cm^{-2}, $\tau_2 = 10$ fs, and $t_{12} = 110$ fs. The SEID simulations were performed for s=1 (●), s=2 (○), s=4 (□), s=8 (△), and s=16 (◇). The s=1 data correspond to the MD simulation. The solid line connecting the MD data was drawn to guide the eye. The inset shows the radial profiles of the local density $\rho \equiv \rho(r,t)$ (at t=233 fs) and of the CM collision energy $E_{CM} \equiv E_{CM}(r,t)$ (at t=233 fs), which manifest the formation of an overrun shell near the cluster periphery.

In Fig. 6 we portray the SEID simulation results for $\bar{E}_{CM}(t)$, Eq. (A2), for INTRA collisions in the intermediate size $(D_2)_N$ cluster ($R_0 = 40$ Å), which were obtained using the following values for the scaling parameter: s=1, 2, 4, 8, and 16. The parameters for the two-pulse irradiation were taken as $I_1 = 5 \times 10^{14}$ W cm^{-2}, $\tau_1 = 10$ fs, $I_2 = 10^{18}$ W cm^{-2}, $\tau_2 = 10$ fs, and $t_{12} = 120$ fs. Consider first the $\bar{E}_{CM}(t)$ versus t curve for the most accurate MD calculation with s=1 (Fig. 6). Up to the onset of the second pulse at t=110 fs the CM collision energy is small, representing a background noise. At t>120 fs, $\bar{E}_{CM}(t)$ begins to increase, reaching a maximum of $\bar{E}_{CM}(t) = 8.1$ eV at t=220 fs. The radial profiles of the local atom density $\rho(r,t)$ and of the CM collision energy for radial ion motion $E_{CM}(r,t)$, Eq. (A1), are shown in the inset of Fig. 6 for time t=233 fs, i.e., in the vicinity of the maximum in $\bar{E}_{CM}(t)$. Both $\rho(r,t)$ and $E_{CM}(r,t)$ (at t=233 fs) are small and roughly constant (with fluctuations due to statistical origin) over the entire interior volume of the exploding cluster. Near the cluster periphery $\rho(r,t)$ and $E_{CM}(r,t)$ (at t=233 fs) steeply increase and then decrease with increasing r, clearly demonstrating the presence of a thin overrun shell (inset of Fig. 6).

For large values of s, significant deviations between the SEID data and the MD data (s=1) are exhibited. For s=16 the maximum in $\bar{E}_{CM}(t)$ is considerably higher than for the MD simulation result (s=1) and is shifted to a lower value of t (Fig. 6). For s=8 the deviations between the SEID data and

the MD data (s=1) are less pronounced, with the position of the maxima being nearly identical for the two procedures. The SEID simulation results for $s \leq 4-8$ converge to the MD s=1 data with near independence of the CM energies on the scaling parameter s, with deviations of ~20% in the vicinity of the maximum in $\bar{E}_{CM}(t)$. The validity range for the applicability of the SEID procedure for CM collision kinetic energies in the intermediate sized cluster ($n=1.289\times10^4$) is characterized by $s/n \leq 3\times10^{-4}$. This s/n value for the validity range for the applicability of the SEID for INTRA collisions within an exploding intermediate sized cluster, which was inferred from the simulations of $\bar{E}_{CM}(t)$, is similar to that estimated by the empirical extrapolation method for INTRA fusion yields within an exploding nanodroplet (Sec. III and Fig. 2).

[1] V. P. Krainov and M. B. Smirnov, Phys. Rep. **370**, 237 (2002).
[2] A. Heidenreich, I. Last, and J. Jortner, Proc. Natl. Acad. Sci. U.S.A. **103**, 10589 (2006).
[3] F. Peano, J. L. Martins, R. A. Fonesca, F. Peinetti, R. Mulas, G. Coppa, I. Last, J. Jortner, and L. O. Silva, Plasma Phys. Controlled Fusion **50**, 124049 (2008).
[4] J. Zweiback, R. A. Smith, T. E. Cowan, G. Hays, K. B. Wharton, V. P. Yanovsky, and T. Ditmire, Phys. Rev. Lett. **84**, 2634 (2000).
[5] I. Last and J. Jortner, Phys. Rev. Lett. **87**, 033401 (2001).
[6] I. Last and J. Jortner, Phys. Rev. Lett. **97**, 173401 (2006).
[7] I. Last and J. Jortner, Phys. Rev. A **77**, 033201 (2008).
[8] A. E. Kaplan, B. Y. Dubetsky, and P. L. Shkolnikov, Phys. Rev. Lett. **91**, 143401 (2003).
[9] F. Peano, R. A. Fonseca, and L. O. Silva, Phys. Rev. Lett. **94**, 033401 (2005).
[10] F. Peano, R. A. Fonseca, J. L. Martins, and L. O. Silva, Phys. Rev. A **73**, 053202 (2006).
[11] G. Grillon, Ph. Balcou, J.-P. Chambaret, D. Hulin, J. Martino, S. Moustaizis, L. Notebaert, M. Pittman, Th. Pussieux, A. Rousse, J.-Ph. Rousseau, S. Sebban, O. Sublemontier, and M. Schmidt, Phys. Rev. Lett. **89**, 065005 (2002).
[12] K. W. Madison, P. K. Patel, D. Price, A. Edens, M. Allen, T. E. Cowan, J. Zweiback, and T. Ditmire, Phys. Plasmas **11**, 270 (2004).
[13] S. Karsch, S. Düsterer, H. Schwoerer, F. Ewald, D. Habs, M. Hegelich, G. Pretzler, A. Pukhov, K. Witte, and R. Sauerbrey, Phys. Rev. Lett. **91**, 015001 (2003).
[14] S. Ter-Avetisyan, M. Schnürer, D. Hilscher, U. Jahnke, S. Busch, P. V. Nicles, and W. Sandner, Phys. Plasmas **12**, 012702 (2005).
[15] I. Last and J. Jortner, Phys. Rev. A **64**, 063201 (2001).
[16] I. Last and J. Jortner, J. Phys. Chem. A **106**, 10877 (2002).
[17] P. B. Parks, T. E. Cowan, R. B. Stephens, and E. M. Campbell, Phys. Rev. A **63**, 063203 (2001).
[18] J. Zweiback, T. E. Cowan, J. H. Hartley, R. Howell, K. B. Wharton, J. K. Crane, V. P. Yanovsky, G. Hayes, R. A. Smith, and T. Ditmire, Phys. Plasmas **9**, 3108 (2002).
[19] J. Davis, G. M. Petrov, and A. L. Velikovich, Phys. Plasmas **13**, 064501 (2006).
[20] F. Peano, J. L. Martins, R. A. Fonseca, L. O. Silva, G. Coppa, F. Peinetti, and R. Mulas, Phys. Plasmas **14**, 056704 (2007).
[21] H. Li, J. Liu, Ch. Wang, G. Ni, Ch. J. Kim, R. Li, and Zh. Xu, J. Phys. B **40**, 3941 (2007).
[22] E. Barkai, Y. Yung, and R. Silbey, Annu. Rev. Phys. Chem. **55**, 457 (2004).
[23] H. Lu, L. Xun, and X. S. Xie, Science **282**, 1877 (1998).
[24] I. Last and J. Jortner, Phys. Rev. A **71**, 063204 (2005).
[25] C. K. Birdshall and A. B. Langdon, *Plasma Physics via Computer Simulation* (McGraw-Hill, New York, 1985).
[26] I. Last and J. Jortner, Phys. Rev. A **75**, 042507 (2007).
[27] I. Last and J. Jortner, Phys. Rev. A **73**, 013202 (2006).
[28] I. Last and J. Jortner, J. Chem. Phys. **121**, 3030 (2004).
[29] I. Last, J. Jortner, F. Peano, and L. P. Silva, "Overrun effects in nuclear fusion within a single Coulomb exploding nanodroplet," Eur. Phys. J. D (in press, 2010).
[30] These "shock shells" (Refs. 8–10), which were also referred to as "thin shells" in CE of heteronuclear CaNs (Ref. 24), do not manifest shock-wave phenomena (Ref. 24).
[31] D. J. Rose and M. Clark, Jr., *Plasmas and Controlled Fusion* (MIT, Cambridge, 1961), p. 13.
[32] I. Last and J. Jortner, J. Chem. Phys. **120**, 1336 (2004).
[33] A. Heidenreich, I. Last, and J. Jortner, Isr. J. Chem. **47**, 89 (2007).
[34] B. N. Breizman and A. V. Arefiev, Plasma Phys. Rep. **29**, 593 (2003).
[35] A. Heidenreich, I. Last, and J. Jortner, Eur. Phys. J. D **46**, 195 (2008).
[36] I. Last and J. Jortner, Phys. Plasmas **14**, 123102 (2007).
[37] Y. Youssef, R. Kodama, H. Habara, K. A. Tanaka, Y. Sentoku, M. Tampo, and T. Toyama, Phys. Plasmas **12**, 110703 (2005).